УДК 544.77.022.532+ 544.723.23+54-438+004.942

SOLVATOCHROMIC REICHARDT'S DYE IN MICELLES OF SODIUM CETYL SULFATE: MD MODELING OF LOCATION CHARACTER AND HYDRATION

V.S. Farafonov, A.V. Lebed, N.O. Mchedlov-Petrossyan

Properties of the standard solvatochromic Reichardt's dye in micelles of sodium cetyl sulfate at 50°C were investigated by means of molecular dynamics simulations. The characteristics of the localization and orientation of the dye molecule as well as its microenvironment were obtained. The calculated characteristics were compared with those in micelles of sodium dodecyl sulfate at 50°C and 25°C as well as with those in micelles of cetyltrimethylammonium bromide at 25°C. The localization, orientation and hydration of the dye in both anionic micelles at both temperatures were found similar and moderately different from those in the cationic micelles. The impact of the hydrocarbon tail length and headgroup nature on these characteristics is discussed.

Keywords: solvatochromism, polarity, sodium cetyl sulfate, sodium dodecyl sulfate, cetyltrimethylammonium bromide, localization, orientation, hydration, molecular dynamics simulation.

Introduction

Solvatochromic dyes are successfully employed for examining various media ranging from pure and mixed solvents to colloid solutions. One of the most suitable and commonly used dyes is 4-(2,4,6-triphenylpyridinium-1-yl)-2,6-diphenylphenolate, known as the standard solvatochromic Reichardt's dye (RD). The information about the polarity of the medium is obtained from the spectrum of the dye dissolved in it, because this spectrum strongly depends on the dielectric constant and hydrogen bonds donating ability of the microenvironment of the dye molecule and, especially, its O atom that is a single hydrogen bonds acceptor in the molecule [1–3]. Consequently, the polarity parameter of the medium, which is denoted $E_T(30)$, is calculated from the wavelength of the maximum in the visible portion of the spectrum, λ_{max}:

$$E_T(30) = hcN_A / \lambda_{max}$$

The more convenient normalized polarity parameter, E_T^N, is also often used. It equals 1.000 for highly polar water and 0.000 for nonpolar tetramethylsilane:

$$E_T^N = [E_T(30) - 30.7] / 32.4$$

However, the treatment of polarity parameters of colloid solutions is complicated by the highly inhomogeneous character of the dye molecule microenvironment. In general outline, the dye is situated in the surface layers of micelles, which are quite thin (<1 nm). Thus, in various micelles, the RD molecule can sense different areas of the surface layer that would make obtained $E_T(30)$ values incomparable. Therefore, this application requires deeper understanding of the microscopic structures of the described dye–micelle systems [4,5].

In this study, we employ the method of molecular dynamics (MD), which would give an insight into the properties of these systems on the molecular level. Previously, we have studied the character of location of RD in micelles of sodium *n*-dodecyl sulfate (or lauryl sulfate), SDS, and *n*-hexadecyltrimethylammonium (cetyltrimethylammonium) bromide, CTAB, dispersed in water [6]. These surfactants were selected as the most popular ones both in academic research and applied science. Interestingly, sodium cetyl sulfate, SCS, having the same length of the hydrocarbon tail as CTAB, is not widely used. The reason is just its high Krafft temperature [4]. It means that in water, micelles of this surfactant are formed only at temperature around 50°C or higher.

In Table 1, the experimental data are set out demonstrating the peculiar of the behavior of RD in the aforesaid micellar systems [4]. The "apparent" pK_a^{app} values refer to the dissociation of the colorless cationic form of the dye to the colored zwitterion and H^+ ion.

Now, it is important to understand if the previously revealed differences in the location and hydration of the dye on SDS and CTAB micelles are caused only by the different charge of the amphiphile ion, or the length of the tail also plays some role. Therefore, we continued our MD modelling by ex-

amining Reichardt's dye in SCS micelles at 50°C. We will compare our findings with the properties of the dye in micelles of CTAB and SDS, which will allow us to separate the influences of the headgroups nature and the tail length on the microenvironment of the adsorbed dye. To improve the reliability of the comparison and gain an additional insight, we repeated the simulation of the RD in SDS micelles at the same temperature, as in SCS micelles (50°C). Running ahead, we considered simulating RD in CTAB micelles at 50°C as unneeded after examination of the obtained results.

Table 1. The absorption maxima and indices of apparent dissociation constant of the solvatochromic RD indicator in water and micellar solutions.

surfactant (0.01 M)	t, °C	λ_{max}, nm	E_T^N	pK_a^{app} (0.05 M NaCl)
none (water)	25	453	1.000	8.64
none (water) [7]	50	460	0.969	–
SDS	25	497	0.828	10.70 ± 0.01
SDS	50	502	0.810	10.61 ± 0.04
SCS	50	510	0.783	10.47 ± 0.07
CTAB	25	540	0.687	7.42 ± 0.02

Potential models

The models for surfactants were taken from our previous works [8,9]. They were developed in the framework of the widely used and well-validated OPLS-AA force field [10]. The dye was parametrized in accordance to the recommended OPLS-AA methodology in order to ensure the mutual compatibility of all used potential models. Because of the complex electronic structure of the dye molecule, we computed atomic point charges anew instead of using the standard force field ones. The first stage was the quantum chemical geometry optimization on RHF level of theory using the 6-31G(d) basis set. On the second stage, the distribution of the electrostatic potential around the molecule was fitted by means of a system of atom-centered point charges using the CHELPG algorithm. In order to obtain reliable values, we employed the RED server to automate the process [11]. The parameters for phenyl-phenyl bonds were taken from the paper by Dahlgren et al. [12].

Simulation methodology

All simulations were carried out using GROMACS 5 [13] software package. The following parameters were used: temperature of 323 K and pressure of 1 bar, which were maintained by means of Berendsen couplings with the thermostat time constant of 1 ps and the barostat time constant of 1.5 ps, the time step of 2 fs for SDS or 1.6 fs for SCS and CTAB, the 3D periodic boundary conditions, the PME method for electrostatics, the cut-off of the van der Waals interactions with the radius of 1 nm, constraints on all covalent bonds.

The initial structure was a water box containing a micelle with a solubilized dye molecule. The aggregation numbers were chosen 60 for SDS and 80 for SCS to correspond the ones of SDS and CTAB micelles examined in our previous work. For each system, three different initial configurations were prepared, and for each, a 90 ns simulation was performed. The first 10 ns of the trajectories were not accounted for in computations because of the relocation of the molecule from the micelle interior to the surface during this time interval.

Results and discussion

The basic characteristics of the system structure are radial distribution functions (RDFs) between its components. We calculated RDFs between micelle center of mass (COM) and O and N atoms of the dye molecule, which show the preferable location of the dye, and compared them with RDFs micelle COM — surfactant headgroup S (N) atoms, which indicate the ranges of the surface layer, Fig. 1.

It could be seen that in SCS micelles, the dye is located significantly closer to the water phase than in CTAB ones. At the same time, the distances between the O peak and the headgroups peak in SCS and SDS micelles at 50 °C are close, which is also true for the N peak. This indicates that in both alkyl sulfate micelles, the dye is localized in the same region of the surface layer. Therefore we can con-

clude that the length of the hydrocarbon tail does not affect the localization of the dye molecule, while the headgroup nature is of main importance.
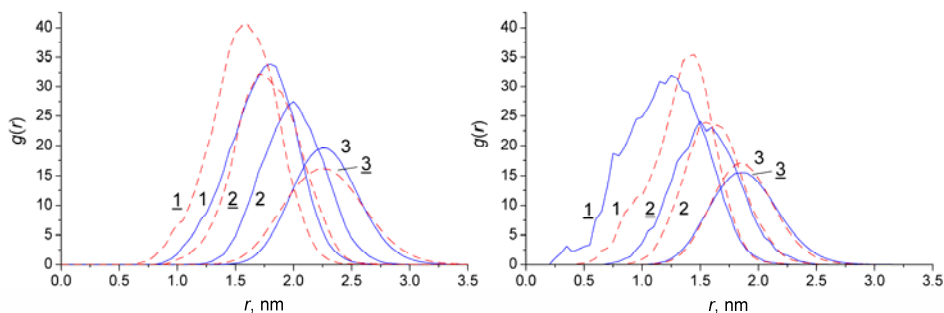

Figure 1. Left: Radial distribution functions in SCS solution (solid curves), compared to RDFs in CTAB solution (dashed curves, underlined numbers). Right: RDFs in SDS solution at 50°C (solid curves) and at 25°C (dashed curves, underlined numbers). RDFs micelle COM – N, micelle COM – O, micelle COM – surfactant S (N) are numbered 1, 2, 3, respectively.

In all cases, the N peak is located behind the O peak. This corresponds to the inclined orientation of the dye molecule, having the pyridinium part immersed into micelle notably deeper than the phenolate part. Interestingly, in the SDS solution at 50 °C, the N peak is widened and shifted to the micelle center, compared to the same solution at 25 °C. This shows the increased probability of deep penetration of the pyridinium part of the molecule in the micelle. The O peak is changed to a much lesser extent, which means that the phenolate part remains located on the micelle surface.

We make a note that the studied micelles have not a spherical but an ellipsoidal shape. This introduces some ambiguity in the presented RDFs because the surface of a micelle is actually located on a range of distances from its COM, which causes moderate widening of the peaks.

For description of the orientation of the dye molecule, we plotted the probability distribution of the angle θ defined as the angle between vectors micelle COM — RD N and RD N atom — RD O, Fig. 2. The right angle corresponds to the orientation parallel to the micelle surface, while deviations show some inclination of the molecule. The values around 0° or 180° correspond to the molecule alignment along the micelle radius.

All solutions of alkyl sulfates have the same position of the main peak (~74°) and close curves, while in the CTAB solution, the distribution is distinctly shifted on ~8° towards higher θ values. This shows the similarity of the dye molecule orientations in the alkyl sulfate micelles regardless the hydrocarbon tail length, and that the orientation in CTAB micelles is moderately different. For the SDS 50°C solution, the deeper penetration of the pyridinium part in the micelle expresses in the increased appearance of the strongly inclined orientation that corresponds to the minor maximum at ~26°.
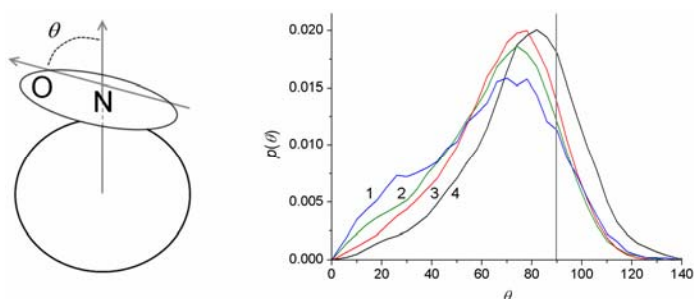

Figure 2. Left: definition of the angle θ, right: probability distribution of θ. 1 — SDS 50°C solution, 2 — SDS 25°C solution, 3 — SCS 50°C solution, 4 — CTAB 25°C solution.

Finally, benefiting from the opportunities of the MD method, we supplement the provided statistical characteristics with easy to understand pictures of the dye location in micelles, extracted from MD trajectories (Appendix, Fig. 1).

Next, in order to establish the connection between the localization of RD and the polarity parameter of the corresponding micellar solution, we revealed the microenvironment of the dye molecule on

considered micelles. The atoms located within 0.4 nm of any dye atom were counted up and classified into 4 categories (micelle hydrocarbon core, surfactant headgroups, water, counterions). The obtained numbers are listed in Table 2 and depicted in Fig. 3. In pure water solutions, there are 215.39 ± 0.08 and 207.0 ± 0.16 atoms around the dye molecule at 25°C and 50°C, respectively. It could be seen that predictably, the total number of atoms in dye microenvironment is roughly similar in various media.

In order to elucidate the connection between the hydration of the O atom with its spectrum, in Table 3 we also collected the E_T^N parameters of the studied solutions together with the numbers of water atoms around the RD O atom, N_w, which is a direct measure of the hydration of the dye O atom in the medium.

Table 2. Average numbers of various atoms in microenvironments of the whole dye molecule and its O atom on different micelles.

surfactant	micelle core	water	headgroups	counterions	total
the dye molecule					
SDS, 25°C	120 ± 5	89 ± 5	8.4 ± 0.7	0.37 ± 0.03	218 ± 11
SDS, 50°C	123 ± 3	79 ± 4	7.2 ± 0.3	0.38 ± 0.011	210 ± 7
SCS, 50°C	119 ± 2	81 ± 2	6.7 ± 0.2	0.347 ± 0.008	207 ± 4
CTAB, 25°C	132 ± 3	65 ± 4	17.0 ± 0.3	0.34 ± 0.016	214 ± 7
the O atom					
SDS, 25°C	2.6 ± 0.17	10.30 ± 0.04	0.032 ± 0.007	0.10 ± 0.02	13.0 ± 0.3
SDS, 50°C	2.27 ± 0.03	9.97 ± 0.09	0.034 ± 0.006	0.10 ± 0.013	12.4 ± 0.14
SCS, 50°C	2.1 ± 0.06	9.94 ± 0.11	0.024 ± 0.003	0.101 ± 0.004	12.1 ± 0.18
CTAB, 25°C	3.9 ± 0.10	5.06 ± 0.06	4.5 ± 0.16	<0.01	13.5 ± 0.3

Table 3. Hydrations of the dye O atom, N_w, and E_T^N parameters in micellar solutions.

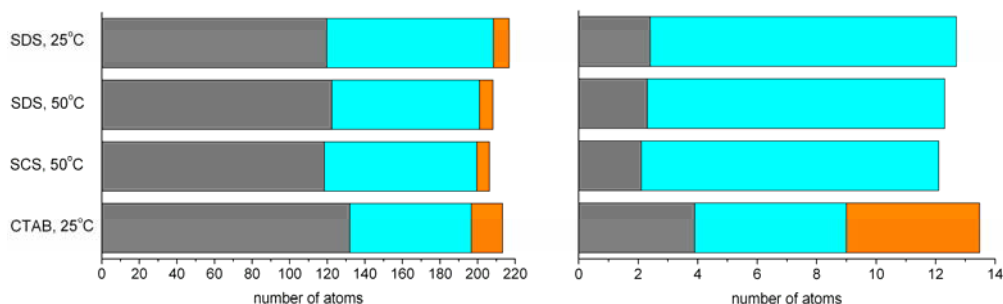| surfactant	N_w	$N_w/N_{w\text{ (water, 25°C)}}$	E_T^N
none (water), 25°C	12.72	1.000	1.000
none (water), 50°C	12.44	0.978	0.969
SDS, 25°C	10.30	0.810	0.828
SDS, 50°C	9.97	0.784	0.810
SCS, 50°C	9.94	0.781	0.783
CTAB, 25°C	5.06	0.398	0.687

Figure 3. Average numbers of various atoms in microenvironments of the whole dye molecule (left) and the O atom (right). The sections of bars correspond to (left to right): the micelle core atoms (gray), the water atoms (cyan), the headgroup atoms (orange).

The microenvironment of the dye molecule and especially its O atom in CTAB micelles appears drastically different from that in SCS micelles. This allowed us suppose that this difference will be preserved at 50°C and, thus, omit the corresponding time-demanding simulation. On the contrary, in all sulfate micelles, the microenvironment is very similar, despite the peculiarity of the dye orientation in SDS micelle at 50°C. The notable feature is the significant (~10%) decreasing of the overall dye

hydration when the temperature increases from 25°C to 50°C. The hydration of the O atom also falls but to the less extent (on 3–4%). This trend is observed for both pure water and SDS dye solutions.

Conclusions

MD simulations of the standard solvatochromic Reichardt's dye in micelles of anionic surfactants sodium cetyl sulfate and sodium dodecyl sulfate at 50°C were performed. The results show similar localizations and orientations of the dye molecule on surfaces of SDS and SCS micelles, which moderately differ from those on surfaces of CTAB micelles. This fact emphasizes the effect of surfactant headgroups on the localization of the RD molecule and shows that the hydrocarbon tail length and, thus, the properties determined by it (micelle size, surface charge density) have rather small influence.

The amount of water around the dye molecule and its O atom were found decreasing with temperature in both SDS and pure water solutions. This fact together with the satisfactory correlation between the N_w value of the dye O atom and the E_T^N value of the solution allow suppose that the difference between the polarity parameters of studied anionic surfactants solutions is to some extent caused by different hydrations of the dye O atom. However, the SCS solution stays somewhat out of this correlation because the hydrations of the whole dye molecule and its O atom in SCS micelle are very close to those in SDS micelle at the same temperature, but the polarity parameter is considerably lower. This could be explained by the significant uncertainties of the N_w values (~0.1) obtained in corresponding simulations despite their considerable length, and by the inaccuracies of the measured E_T^N values.
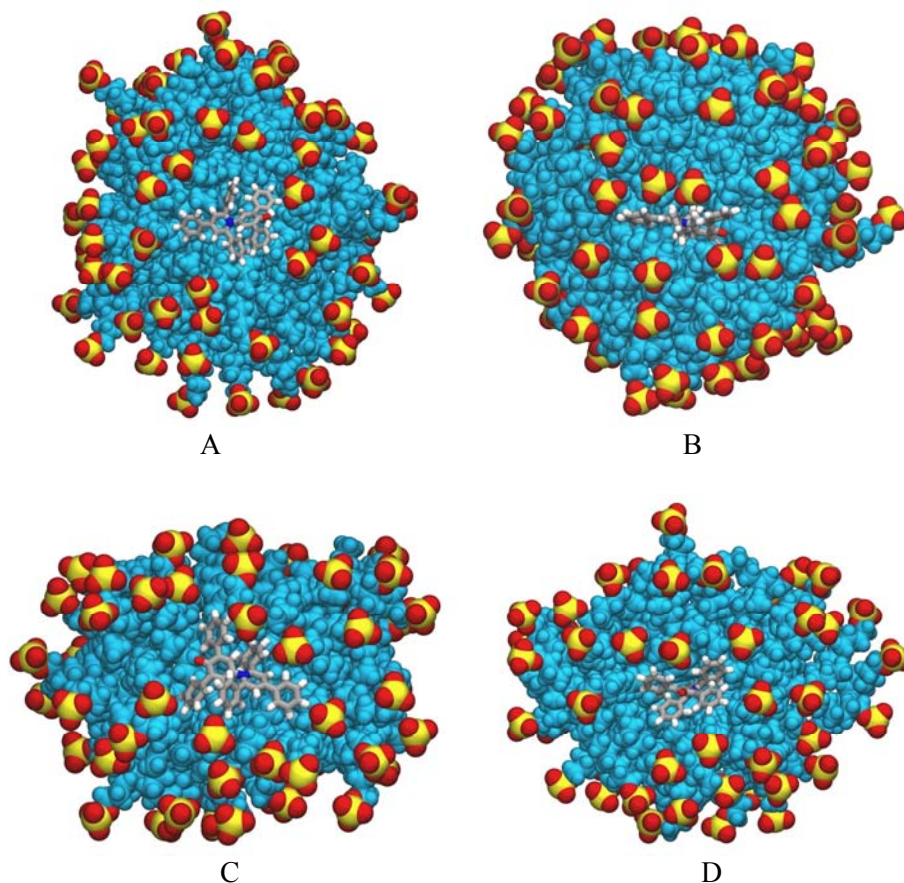
Appendix

Figure 1. Snapshots from MD trajectories showing typical dye localizations in SCS (A, B) or SDS (C, D) micelles at 50°C. In B, the molecule is immersed into the micelle with two *ortho*- phenyl substituents located at the same side of the molecule's symmetry axis, while two other *ortho*- phenyl substituents are situated in the surface layer. In D, the pyridinium part is completely immersed into micelle, and the phenolate part resides in the surface layer. For the SDS solution at 25°C, the orientation shown at D is not typical.

References

1. Machado V. G., Stock R. I., Reichardt C. Pyridinium N-phenolate betaine dyes. // Chem. Rev. 2014. Vol.114. P.10429–10475.
2. Reichardt C., Welton T. Solvents and Solvent Effects in Organic Chemistry. Wiley: New York, 2011.
3. Bosch M., Roses E. Relationship between ET polarity and composition in binary solvent mixtures. // J. Chem. Soc., Faraday Trans. 1992. Vol.88. P.3541–3546.
4. Mchedlov-Petrossyan N. O. Protolytic equilibrium in lyophilic nanosized dispersions: differentiating influence of the pseudophase and salt effects. // Pure Appl. Chem. 2008. Vol. 80. P.1459–1510.
5. Drummond C.J., Grieser F., Healy T. W. A single spectroscopic probe for the determination of both the interfacial solvent properties and electrostatic surface potential of model lipid membranes. // Faraday Discuss. Chem. Soc. 1986. Vol.81. P.95–106.
6. Farafonov V. S., Lebed A. V., Mchedlov-Petrossyan N. O. Character of localization and microenvironment of the solvatochromic Reichardt's betaine dye in SDS and CTAB micelles: MD simulation study. // Langmuir 2017. Vol.33, No.33. P.8342–8352.
7. Liotta C. L., Hallett J. P., Pollet P., Eckert C. A. Reactions in nearcritical water. In: Organic reactions in water: principles, strategies and applications. Edited by Lindstrom U. M. Blackwell publishing: Oxford, UK.
8. Farafonov V. S., Lebed A. V. Developing and validating a set of all-atom potential models for sodium dodecyl sulfate. // J. Chem. Theory Comp. 2017. Vol.13, No.6. P.2742–2750.
9. Farafonov V. S., Lebed A. V. Molecular dynamics simulation study of cetylpyridinum chloride and cetyltrimethylammonium bromide micelles. // Kharkov Univ. Bull., Chem. Ser. Vol.2016. P.25–30.
10. Jorgensen W.L., Maxwell D.S., Tirado-Rives J. Development and Testing of the OLPS All-Atom Force Field on Conformational Energetics and Properties of Organic Liquids. // J. Am. Chem. Soc. 1996. Vol.118, No.15. P.11225–11236.
11. Vanquelef E., Simon S., Marquant G., Garcia E., Klimerak G., Delepine J.C., Cieplak P., Dupradeau F.-Y. R.E.D. Server: a web service for deriving RESP and ESP charges and building force field libraries for new molecules and molecular fragments. // Nucleic Acids Res. 2011. Vol.39. P.511–517.
12. Dahlgren M. K., Schyman P., Tirado-Rives J., Jorgensen W. L. Characterization of biaryl torsional energetics and its treatment in OPLS all-atom force fields. // J. Chem. Inf. Model. 2013. Vol.53. P.1191–1199.
13. Abraham M.J., Murtola T., Schulz R., Pall S., Smith J.C., Hess B., Lindahl E.. GROMACS: High performance molecular simulations through multi-level parallelism from laptops to supercomputers. // SoftwareX. 2015. Vol.1–2. P.19–25.

В.С. Фарафонов, А.В. Лебедь, Н.О. Мчедлов-Петросян. Сольватохромный краситель Райхардта в мицеллах цетилсульфата натрия: МД моделирование характера локализации и гидратации.

Свойства стандартного сольватохромного красителя Райхардта на мицеллах цетилсульфата натрия при 50°C исследованы с помощью молекулярно-динамического моделирования. Получены характеристики локализации и ориентации молекулы красителя и ее микроокружения. Они сопоставлены с характеристиками молекулы красителя на мицеллах додецилсульфата натрия при 50°C и 25°C и бромида цетилтриметиламмония при 25°C. Локализация, ориентация и гидратация красителя на обеих анионных мицеллах при обеих температурах найдены близкими и умеренно отличными от таковых на катионных мицеллах. Обсуждено влияние длины углеводородного радикала и природы головных групп на рассмотренные характеристики.

Ключевые слова: сольватохромизм, полярность, цетилсульфат натрия, додецилсульфат натрия, бромид цетилтриметиламмония, локализация, ориентация, гидратация, молекулярно-динамическое моделирование.

В.С. Фарафонов, О.В. Лебідь, М.О. Мчедлов-Петросян. Сольватохромний барвник Райхардта в міцелах цетилсульфату натрію: МД моделювання характеру локалізації та гідратації.

Властивості стандартного сольватохромного барвника Райхардта на міцелах цетилсульфату натрію при 50°C досліджені за допомогою молекулярно-динамічного моделювання. Отримані характеристики локалі-зації та орієнтації молекули барвника та її мікрооточення. Вони порівняні із характеристиками молекули барвника на міцелах додецилсульфату натрію при 50°C і 25°C та броміду цетилтриметиламонію при 25°C. Локалізація, орієнтація та гідратація барвника на обох аніонних міцелах при обох температурах знайдені близькими та помірно відмінними від таких на катіонних міцелах. Обговорений вплив довжини вуглеводне-вого радикалу та природи головних груп на розглянуті характеристики.

Ключові слова: сольватохромізм, полярність, цетилсульфат натрію, додецилсульфат натрію, бромід цетилтриметиламонію, локалізація, орієнтація, гідратація, молекулярно-динамічне моделювання.